Modelling Human Gait using a Nonlinear Differential Equation

Jelena Schmalz[1,*], David Paul[1], Kathleen Shorter[1], Matthew Cooper[1], Aron Murphy[1]

1 University of New England, NSW, Australia

Current Address: School of Science & Technology, Armidale, UNE, Australia
* jschmalz@une.edu.au

Abstract

We introduce an innovative method for the investigation of human gait, which is based on the visualisation of the vertical component of the movement of the centre of mass during walking or running, in the space of the coordinates position, velocity, and acceleration of the centre of mass. Collected data has been numerically approximated by the best fitting plane for a linear model and by the best fitting curve for a non-linear model. The resulting equation for the best fitting plane or curve in this space is a differential equation of second order. The model that we suggest is a Duffing equation with coefficients that depend on the height of a walker or runner and on the angular frequency of the oscillation. Solutions to those Duffing equations have been compared with the data, both visually and by computing the mean squared error. Future plans for applications of the new method are proposed.

1 Author Summary

We study the human gait modelled by the movement of the centre of mass of the test person. This is an example of a biological process which can be considered as a periodical dynamic system. Roughly, this movement behaves in a similar way as a vibrating mass suspended on a spring, but it is more complex. The vertical component of the movement during walking or running can be visualised as an oscillogram: a graph of the position as a function of time. We suggest a visualisation of the data in 3D space, where the coordinates describe position, velocity, and acceleration. Our new visualisation method allows us to model the movement of a person's centre of mass by a nonlinear differential equation. The resulting curve for an ideal spring-mass movement, without viscosity or external force, is an ellipse in the suggested 3D space. The shape of the data curve shows at which position an additional force was applied, or the movement has slowed down. Some deviations are common for all test persons and others are different. In the future we plan to investigate the reasons for these deviations, such as different running techniques or injuries.

2 Introduction

2.1 Background

The research on the mechanics of human gait can be of interest for different disciplines, for example sport science, medicine, and robotics. In this paper we discuss a model for the movement of the vertical coordinate of the centre of mass (COM) during walking and running.

Human locomotion is an inherently complicated process requiring the complex integration of neural and musculoskeletal control in response to both internal and external forces. In an attempt to strip away complexity and gain an understanding of the fundamental principles underpinning human locomotion, simple mechanical models have been developed. The mechanical simplification of locomotion allows the identification of just a few key parameters that can be manipulated to examine cause and effect relationships and identify which features most influence the system [1, 2].

Blickhan suggested a linear spring-mass model for hopping in 1989, [3], other papers followed, for example [4–7]. The motion of the centre of mass is described by the equation $mz_{tt} + Kz = -mg$, where m is the body mass, z is the vertical deflection of the centre of mass with the origin on the treadmill surface and the direction chosen upwards. The constant K is the stiffness, and g is gravitational acceleration. By z_{tt} we denote the second derivative of z, i.e. the vertical acceleration of the centre of mass.

There have been different approaches on how to calculate leg stiffness. Blickhan's approach uses the formula $K = m\omega_0^2$, where ω_0 is the stride's angular frequency of the oscillation, which, during gait reflects the stride's angular frequency. [3, 6].

The other approach for calculation of the leg stiffness is to find the ratio of F_{max}, the maximum value of the vertical ground reaction F_{max} force, and ΔL, the absolute value of the leg compression, i.e. $K = \frac{F_{max}}{\Delta L}$. This definition of leg stiffness is used in papers [4, 5, 7–9]. An overview of these two approaches is presented in [6]. There is a third approach to leg stiffness calculation based on the measurements of loss of mechanical energy by walking/running, W. Leg stiffness K is found from the formula $W = \frac{1}{2}K(\Delta r)^2$, where Δr is the shortening of a spring (e.g. [10]).

In examining mechanical and metabolic determinants of the human walking gait, Kuo [11], and [12] employed an anthropomorphic three-dimensional, passive-dynamic model, in which human legs were represented as rigid inverted pendulums with small point masses modelling each foot and a larger mass modelling the concentration of the COM at the pelvis. These studies drew on earlier models of a rigid swing leg during walking [13] and continued the view that walking and running were two distinct gaits that could not be described using similar mechanical models. This view, however, was discounted by Geyer, Seyfarth, Blickhan (2006) [14] who demonstrated that a compliant-legged, spring-mass bipedal model consisting of two linear, equal and massless springs and a single COM point mass, as an extension of Blickhan's one-dimensional model, reliably predicted ground reaction forces and COM behaviour in both human walking and running. Several subsequent studies further validated the efficacy of a bipedal spring-mass model of walking [2, 15–18]. While Blickhan's planar spring-mass model remains largely valid and has been applied, with modifications to suit certain parameters, in recent studies [19, 20], much of the twenty-first century research in the field has adopted the bipedal spring-mass model and focused on adapting or adding selected elements to improve prediction accuracy for both walking and running gait mechanics. Investigations have considered the effects of varying points of force application [1, 16], changes in leg stiffness depending on walking/running speed [15, 17], variations in touchdown or take-off angle and velocity [2], the effects of swing leg dynamics [18] and indeed, various combinations of these parameters.

In the papers listed above, the starting point for mathematical models was the

consideration of the mechanics of the human gait. We approach the problem from the other side. Our mathematical model is based on the analysis of the collected data of the three dimensional movement of COM. In this paper we concentrate on the projection of the movement of COM on the vertical axis. We plan to collect more data and apply our new method for the investigation of projections on the horizontal axes – the axis along the walking/running movement and the axis that is perpendicular to it, see Section 8.

We suggest a new approach for finding leg stiffness for the simple harmonic oscillation model, and then develop a more precise model assuming that the stiffness for a fixed speed is not a constant but depends on the displacement of COM. The innovative idea of our method is to visualise the data for the vertical component of a motion of the centre of mass, $z(t)$, as a curve in the three dimensional space, (z, z_t, z_{tt}) (see Section 3). Here z_t and z_{tt} are the first and the second derivatives of the function $z(t)$, correspondingly. These curves are interesting by themselves as they are individual for each person and velocity. We provide examples of the variety of these curves in Section 8. In this paper we discuss the properties that are common for these curves. We apply the Fast Fourier Transform filter (FFT) to the data to filter out the smaller frequencies.

2.2 Three models are suggested in our paper

Our mathematical models are based on the collected data, see Section 3. Each suggested model is a modified version of a previous one. The data is placed in the space (z, z_t, z_{tt}) – these curves are interpreted in Section 4. For the linear model (see Section 5) we first find the equation for the best fitting plane in this three dimensional space numerically. We interpret the equation of the plane as a second order differential equation with constant coefficients,

$$mz_{tt} + K(z - z_0) = 0. \tag{1}$$

Here z_0 is the z-coordinate of the centre of the ellipse. The slope of the plane Eq.(1) is equal to the constant $-\frac{K}{m}$. The numerically calculated slope multiplied by the mass of a participant gives us the leg stiffness. The harmonic oscillating model is the same model as suggested by Blickhan, only the method to evaluate leg stiffness is new.

This model does not take into account that, for a fixed walking/running speed, stiffness is not constant. In reality, stiffness is changing throughout the different phases of the gait cycle. Therefore we modify the model. The second model considers a changing stiffness $\mathcal{K}$ that depends on $z(t)$. This leads to a non-linear differential equation, see Section 6). We look for the best fitting curve of the form

$$mz_{tt} + \nu_1 z_t + \nu_2 z_t^2 + \nu_3 z_t^3 + K_1 z + K_2 z^2 + K_3 z^3 + c = 0, \tag{2}$$

with some initial conditions for z and z_t that are extracted from data. Here the term $\nu_1 z_t + \nu_2 z_t^2 + \nu_3 z_t^3$ is the approximation of the damping force, $K_1 + K_2 z(t) + K_3 z^2(t)$ is the approximation of the stiffness function $\mathcal{K}(t)$, and $\nu_1, \nu_2, \nu_3, K_1, K_2, K_3$ are some constants. We have observed that the best fitting curve can be written in the form of a second-order non-linear differential equation with initial conditions $z(0), z_t(0)$,

$$mz_{tt} + Kz(z - z_0)(h - z) = 0, \tag{3}$$

where z_0 is the average height of the COM, and h is the person's height, both measured during walking/running. The constant K is not the same as stiffness in Eq.(1), where it is equal to $m\omega^2$. In Eq.(3), K is approximately equal to $\frac{m\omega^2}{z_0(h-z_0)}$. The second model takes into account the non-constant stiffness, but not the damping and excitation forces. In Section 7 we discuss the third model. It is an approximation by a second order

non-linear non-homogeneous differential equation that considers nonzero damping and excitation forces.

Section 8 gives a short overview of how we plan to apply our new method in further research.

3 Data Recording

We have collected data for six participants aged from 18 to 55 years, three males and three females. The study followed ethical protocols as per ethics requirements (HE19-239). We have measured the vertical coordinates $z(t)$ of the COM for each participant walking or running on the treadmill. The data was collected for different integer velocities, 100 frames per second, during 10 seconds, for each velocity, using an 8 camera, Qualisys Motion capture system with the COM reconstructed using a pelvic marker set within Visual3D.

Using MATLAB, we have visualised the data as curves in the three-dimensional space (z, z_t, z_{tt}). We have filtered out high frequency oscillations, such as noise and individual features, by use of the fast Fourier transform filter function in MATLAB. For FFT threshold equal to 0.3, the curves are close to an ellipse. The direction of the motion along the curve is found, for example, in the following way. Find the point with the greatest z-coordinate. This is the highest point of the centre of mass during the gait cycle. The velocity at this point is equal to zero. Hereafter the movement goes down, i.e. the velocity z_t becomes negative. In both pictures of Figure 1, from those perspectives, the movement is clockwise.

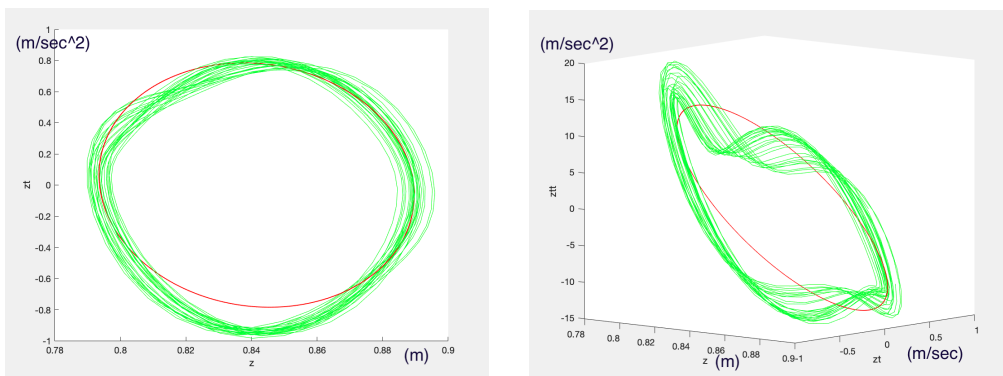

Fig 1. A MATLAB 3D figure shown from different perspectives. The green curve is a smoothed data curve with high-pass filter FFT 0.03, the red curve is a smoothed data with FFT 0.3.

4 Data Interpretation

The pictures in the space with the coordinates position, velocity, and acceleration, are rich in information. For example, Figures 2 and Figure 3 show the data for walking (4km/hr) and running (9km/hr) of a participant, correspondingly. Here we look into

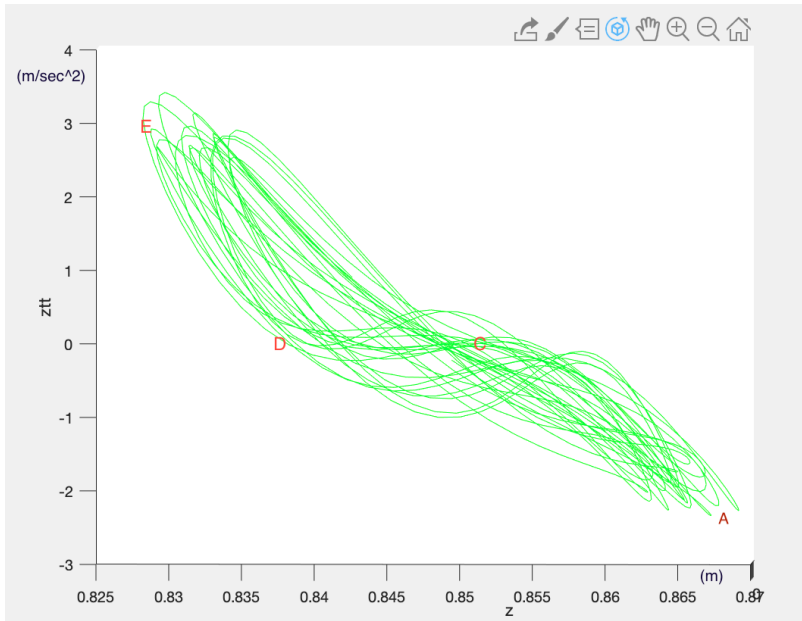

Fig 2. Data for walking, 4km/hr. The horizontal axis shows the position and the vertical axis shows the acceleration of the COM. The part CD corresponds to the phase of the gait when a foot touches the surface, DE corresponds to the propulsion during toe-off, during EA the COM moves upwards and the acceleration diminishes.

the projection to the plane z, z_{tt}, i.e. the horizontal axis shows the position of the COM (in meters) and the vertical axis shows the acceleration (in m/sec^2). The part CD of both curves corresponds to the phase of the gait when a foot touches the surface of the treadmill. In the case of walking it is a flat line, vertical acceleration is close to zero. In the case of running, acceleration is diminishing because of braking during initial foot contact. The phase DE corresponds to the propulsion during toe-off, where acceleration (and consequently force) is increasing. On the segment EA acceleration diminishes, turns to zero when the the COM reaches its average position, and is minimal at the point A. The minimum acceleration for the walking curve is $-2\,m/sec^2$, the minimum acceleration for the running curve is about $-10\,m/sec^2$, i.e. close to the gravitation constant g. The acceleration is less during walking as during running because the body is always in contact with the ground whilst during running there is the flight phase. The arc AB on Figure 3 corresponds to the flight phase of running. This part of the curve is more complicated than just a flat constant $z_{tt} = -g$, because it is smoothly connected with the rest of the curve. Some information that we get from these curves is common for all participants and walking/running speeds, some features are individual – for example not each participant has the "flight" component AB at running speeds, due to individualised transitions between walking and running gait patterns. Our aim in the future is to collect data for more participants and compare individual properties of the curves, see Section 8. In this paper we concentrate on their common properties, and suggest three models, based on differential equations. We build our three models based on data, pure numerically and mathematically. The first model is well-known, it is a

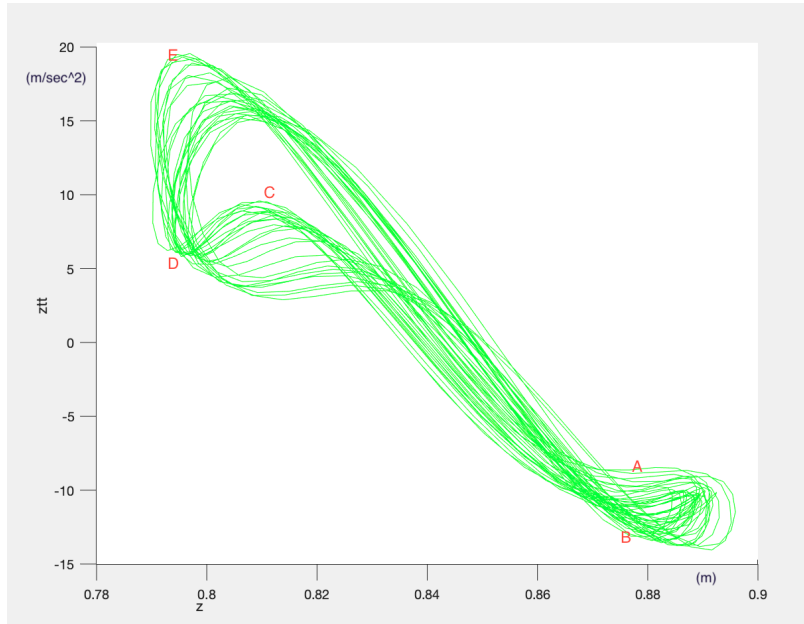

Fig 3. Data for running, 9km/hr. The horizontal axis shows the position and the vertical axis shows the acceleration of the COM. The part CD corresponds to the phase of the gait when a foot touches the surface, DE corresponds to the propulsion during toe-off, during EA the COM moves upwards and the acceleration diminishes. The arc AB corresponds to the flight phase.

harmonic oscillation. Our novelty here is the method that we develop for the computing of stiffness.

5 Modelling Gaits as Harmonic Oscillator

5.1 Best fitting plane and the interpretation of its coefficients

We begin with the visualisation of the data. Consider a curve in the three dimensional space (z, z_t, z_{tt}) that represents smoothed gait data, as for instance the red line on Figure 1 (FFT=0.3). This curve is not quite flat, but it is close to a flat ellipse with the centre at $z = z_0$, $z_t = z_{tt} = 0$. The equation of a plane in three dimensional space (z, z_t, z_{tt}) that passes through the point $(z_0, 0, 0)$ is

$$az_{tt} + bz_t + c(z - z_0) = 0, \tag{4}$$

where a, b, and c are constants, and $z - z_0$ is the vertical displacement of the average of the centre of mass. The zero for $z(t)$ is chosen to be on the level of the treadmill, and the z-axis direction is upwards.

We find the coefficients a, b, and c in the Eq. (4) numerically, by finding the best fitting plane for the smoothed data curve. The equation for the plane is interpreted as a second order differential equation that describes a damped driven harmonic oscillator. The coefficients in Eq. (4), in the context of the spring model, have the meaning of $a = m$, which is the mass of the oscillating object, $b = \nu$, which is the viscosity of the spring, and $c = K$, which is the spring stiffness,

$$mz_{tt} + \nu z_t + K(z - z_0) = 0. \tag{5}$$

In the rest of this section we discuss Eq. (5): the meaning of its coefficients, the solutions, and the connection with the angular frequency of the gait.

The plane given by Eq. (5) intersects the plane (z, z_{tt}) by the straight line $mz_{tt} + K(z - z_0) = 0$, $z_t = 0$. The slope of this line is equal to $-\frac{K}{m}$. Similarly we can find $-\frac{\nu}{m}$ as the slope of the straight line $mz_{tt} + \nu z_t = 0$, $z_{tt} = 0$, in the plane (z, z_t). This gives us a new method to find the stiffness and the viscosity from the numerically computed equation of the best fitting plane.

The coordinate z_0 in Eq. (5) corresponds to the average of the vertical coordinate of the centre of mass and depends on the speed of walker/runner. From the collected data we can observe that z_0 depends on the height, speed, and walking/jogging technique of a participant. Figure 4 represents a typical graph for z_0 depending on the speed of a participant. The vertical coordinate of the centre of mass diminishes with the increasing

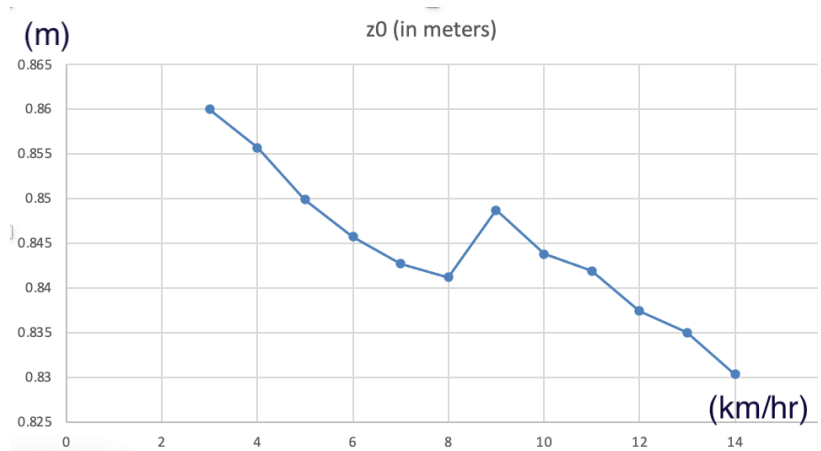

Fig 4. The graph shows the average of the vertical coordinate of the centre of mass, z_0 (in meters) for different speeds (in km/hr), for one participant

speed. The jump between 8 and 9 km/hr corresponds to the transition from walking to running speed.

5.2 Solution to Eq. (5)

Now we discuss the solution to Eq. (5). The discriminant of its characteristic equation is equal to $\nu^2 - 4mK$. If $\nu^2 - 4mK < 0$, which is the case in the gait context, the solutions to the differential equation are

$$z(t) = Ae^{-\frac{\nu t}{2m}} \cos(\omega t - \varphi) + z_0 \tag{6}$$

(see for example Chapter 3 in [21]), where the amplitude A is a nonnegative constant, φ is the phase shift, and the constant ω is the angular frequency, with $\omega^2 = \frac{K}{m}$, (see e.g. [22]). The constants A and φ can be found from the initial conditions.

5.3 Hook's law

If the viscosity is close to zero, $\nu \approx 0$, then $e^{-\frac{\nu t}{2m}} \approx 1$. Otherwise, if $\nu \neq 0$, the curve given by Eq. (6) is not an ellipse but a flat spiral approaching the point $(z_0, 0, 0)$. If we consider a stable gait, we need to assume in this linear model that the viscosity is zero. Eq. (5) turns to

$$mz_{tt} + K(z - z_0) = 0, \tag{7}$$

which is the Hook's Law [23],

$$F(t) = -K(z(t) - z_0). \tag{8}$$

Dividing Eq. (7) by the mass m and applying $\frac{K}{m} = \omega^2$, we get

$$z_{tt} + \omega^2(z - z_0) = 0. \tag{9}$$

Hence, the square of the angular frequency ω^2 can be found as the absolute value of the slope of the plane in Eq. (9). Our calculations for angular frequency using the method above are consistent with the data. Angular frequency in the gait context is the number of steps in one second, multiplied by 2π.

5.4 Leg stiffness as a function of gait frequency

As expected, leg stiffness, and hence angular frequency, increases with an increase of speed. Figure 5 below shows the values of the gate frequencies $fr = \frac{\omega}{2\pi}$ measured in strides per second, for different participants and different speeds. We can observe that

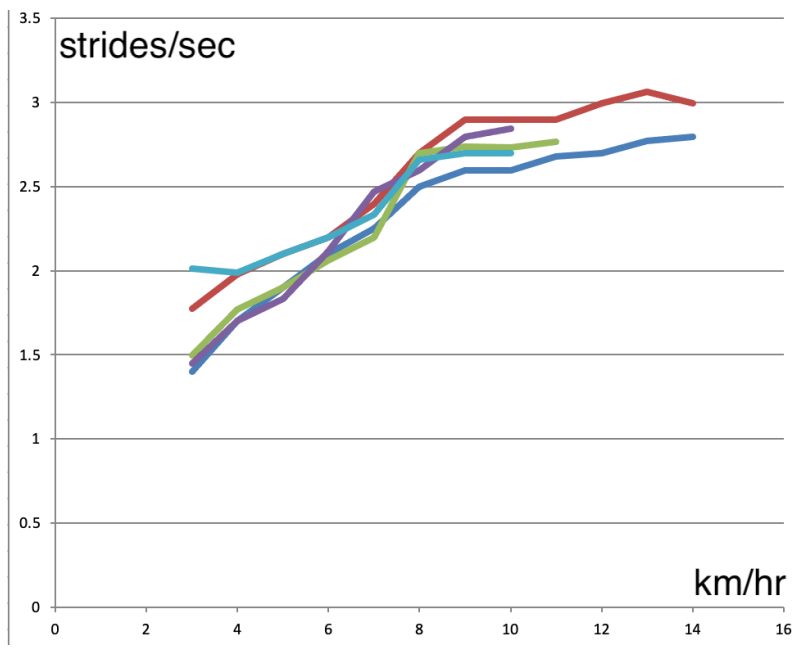

Fig 5. Frequencies fr for different participants (in strides in a second), depending on the walking/running speed

the frequency increases for walking speeds almost linearly, then it increases in a jump by the transition to a running speed, and then it becomes flatter, almost constant.

5.5 Where the gravitation constant is hidden

We note that the gravitation constant is included in Eq. (5) implicitly. Namely, we can rewrite the equation as

$$mz_{tt} + \nu z_t + K(z - z_{st}) = -mg. \tag{10}$$

The coordinate z_{st} is the average of the vertical coordinate of the centre of mass of a standing body but in a walking/running posture, it is not exactly the same as the coordinate of centre of mass in a standing position. The relation between z_0 and z_{st} is calculated from Eqs. (5) and (10) and is $z_0 = z_{st} - \frac{mg}{K}$.

6 Modelling by a non-linear homogeneous differential equation

6.1 Non-linear second order d.e.

In this section we approximate the original curves by a homogeneous non-linear second order differential equation,

$$mz_{tt} + \nu(t)z_t + \mathcal{K}(t)(z - z_0) = 0. \tag{11}$$

Unlike the harmonic oscillation model described in Section 5, we consider stiffness and viscosity to not be constant, but functions depending on time, $\mathcal{K}(t)$ and $\nu(t)$. This makes sense, as stiffness and viscosity depend on a phase of a stride. For example, the slope on Figures 2 and 3 is changing, and the slope in the plane z, z_{tt} reflects stiffness, it is $\frac{\mathcal{K}(t)}{m}$ at a time t. We divide both sides by m and consider the approximation of the functions $v(t) = \frac{\nu(t)}{m}$ and $k(t) = \frac{\mathcal{K}(t)}{m}$ by cubic polynomials,

$$z_{tt} + v_1 z_t + v_2 z_t^2 + v_3 z_t^3 + k_1(z - z_0) + k_2(z - z_0)^2 + k_3(z - z_0)^3 = 0. \tag{12}$$

We look for the best fitting curves of the form

$$z_{tt} + v_1 z_t + v_2 z_t^2 + v_3 z_t^3 + k_1 z + k_2 z^2 + k_3 z^3 + C = 0. \tag{13}$$

This equation is equivalent to Eq. (12) after expanding brackets and renaming coefficients. From our data, the viscosity coefficients v_1, v_2, v_3 turned out to be zero if the FFT threshold is large enough, for instance if it is ≥ 0.3. This is not surprising because we have assumed no excitation force (homogeneous equation), and the participants have maintained stable walking/running.

6.2 Finding and analysing the fixed points

We are also interested in the fixed (equilibrium) points for the curves [22] described by Eq. (13). We first rewrite the second order differential Eq. (12) as a system of first order differential equations:

$$z_t = z_1, \tag{14}$$

$$(z_1)_t = -v_1 z_1 - v_2 z_1^2 - v_3 z_1^3 - k_1 z - k_2 z^2 - k_3 z^3 - C. \tag{15}$$

The fixed points are found by solving the equilibrium equations (see for example [24])

$$z_1 = 0, \tag{16}$$

$$-v_1 z_1 - v_2 z_1^2 - v_3 z_1^3 - k_1 z - k_2 z^2 - k_3 z^3 - C = 0, \tag{17}$$

i.e. the fixed points are the roots of the cubic equation $k_1 z + k_2 z^2 + k_3 z^3 + C = 0$ (we remind that $v_1 = v_2 = v_3 = 0$). The solutions to Eq. (13) are plotted in the same coordinate system as the data curves, see for example the blue and the red curves on Figure 6. The solution curves are stable if we set one fixed point equal to zero, i.e. $C = 0$. Then the two other fixed points occur at z_0 (the centre of the closed curve, average coordinate of the centre of mass), and h, approximately the height of a participant during walking/running. The differential equation Eq. (13) becomes

$$z_{tt} + kz(z - z_0)(h - z) = 0. \tag{18}$$

The connection between the coefficients of Eq. (13) and Eq. 18 is

$$k_1 = -kz_0 h, k_2 = k(h + z_0), k_3 = -k, k > 0, \text{ and } v_1 = v_2 = v_3 = 0. \tag{19}$$

We find the eigenvalues of the Jacobean matrix that occurs from Eqs. (14), (15) and use the standard method for classifying the fixed points. See for example [22]. The Jacobi matrix is

$$J = \begin{bmatrix} 0 & 1 \\ -k_1 - 2k_2 z - 3k_3 z^2 & -v_1 - 2v_2 z - 3v_3 z^2 \end{bmatrix},$$

Substituting the values k_i in terms of z_0 and h, and $v_i = 0$, $i \in \{1, 2, 3\}$ (Eq. (19)), we get

$$J = \begin{bmatrix} 0 & 1 \\ khz_0 - 2k(h + z_0)z + 3kz^2 & 0 \end{bmatrix}.$$

Hence we find the eigenvalues by solving
$\det(J - \lambda I) = \lambda^2 - khz_0 + 2k(h + z_0)z - 3kz^2 = 0$, i.e.

$$\lambda^2 = khz_0 - 2k(h + z_0)z + 3kz^2. \tag{20}$$

Numerical computations show that if we insert $z = 0$ or $z = h$, λ^2 is positive, if $z = z_0$, λ^2 is negative. (It is easy to check on paper that this is true in the case when COM is strictly in the middle, i.e. $h = 2z_0$.) Hence the fixed point $z = z_0$ is a centre, the fixed points $z = 0$ and $z = h$ are saddles. Initial conditions are the values $z(0)$ and $z_t(0)$.

6.3 Example based on the collected data.

Figure 6 shows the observed smoothed data curve (red) and the curve corresponding to the solution of Eq. (18) (blue) for one of the participants, together with the fixed points. The differential equation that describes the movement of the centre of mass of this participant running at the speed 8 km/hr is $z_{tt} + 279(z - 0.9)(1.8 - z) = 0$. We have rounded $|k_3| = k$ to an integer, and z_0 and h to the first decimal place. See Figure 6.

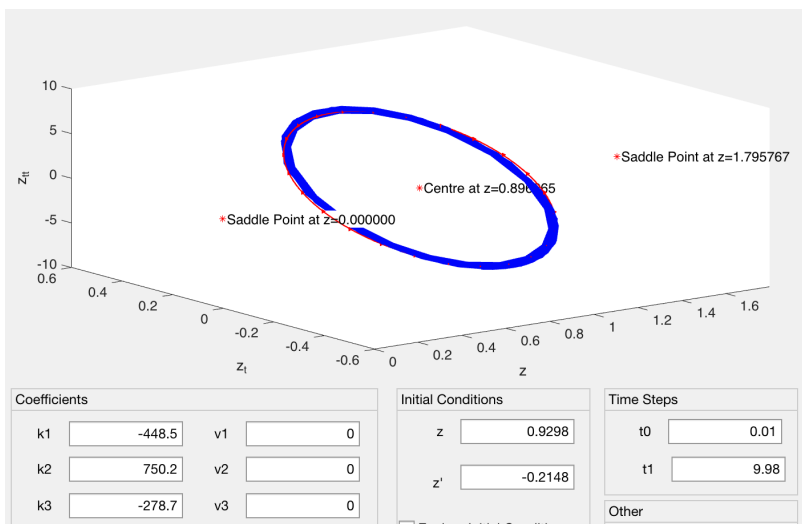

Fig 6. Curve with fixed points and values k_1, k_2, and $k_3 = -k$ for a participant (178cm tall, running at 8 km/h). The mean squared error is 0.015

6.4 Interpretation of the parameters in the model

Eq. (18) shows that we can model the movement of the centre of mass by a Duffing equation, up to a constant k , knowing only a person's height, h, and the z-coordinate of the average of centre of mass, z_0. The height h and z_0 are body measurements in

motion and slightly change for different walking/running speeds (see Figure 4). The gravitation constant g is involved implicitly in the differential equation, in a similar way as in the harmonic oscillation model in Section 5. When the viscosity coefficients are not vanishing, the point $z = z_0$ is a stable spiral instead of a centre.

The coefficient k does not have the meaning of the square of the angular frequency, but k rather behaves in a similar way to leg stiffness: it increases with an increase of the walking/running speed, and depends on the participant. The meaning of the coefficient k is found from the following consideration. We rewrite Eq. (18) as

$$z_{tt} + k[-(z - z_0)^3 + (h - 2z_0)(z - z_0)^2 + z_0(h - z_0)(z - z_0)] = 0. \tag{21}$$

For z close to z_0 the linear approximation at z_0 is

$$z_{tt} + kz_0(h - z_0)(z - z_0) = 0. \tag{22}$$

Comparing this equation with Hook's Law (Eq. (9)) we get an expression that relates the angular frequency ω with the coefficient k and the values z_0 and h:
$\omega^2 \approx kz_0(h - z_0)$. Hence

$$k \approx \frac{\omega^2}{z_0(h - z_0)}. \tag{23}$$

6.5 Case $z_0 = \frac{1}{2}h$

Assuming that the centre of mass is approximately half of the height, $z_0 = \frac{1}{2}h$, and Eq. (21) becomes

$$z_{tt} + kz_0^2(z - z_0) - k(z - z_0)^3 = 0, \tag{24}$$

where $k > 0$, and

$$k = \frac{\omega^2}{z_0^2}. \tag{25}$$

Eq. (24) is the equation for a softening oscillator [24], i.e. the stiffness diminishes with the displacement.

6.6 Hamiltonian and energy level curves

Multiplying both sides of Eq. (24) by z_t and integrating gives the expression for the Hamiltonian,

$$H = \frac{z_t^2}{2} - \frac{k}{4}(z - z_0)^4 + \frac{kz_0^2}{2}(z - z_0)^2. \tag{26}$$

For each constant H we get an energy level curve to Eq. (24) in the phase plane z, z_t. These curves are described by

$$z_t = \pm\sqrt{2H + k\frac{(z - z_0)^4}{2} - kz_0^2(z - z_0)^2}. \tag{27}$$

For Eq. (24) the energy level curves are symmetrical with respect to the horizontal line $z_t = 0$ and with respect to the vertical line $z = z_0$, as we can see from Eq. (27). Figure 7 shows a typical phase space picture with two saddle points and a centre, and corresponding energy levels. In the gate context the initial conditions are closed to z_0, which corresponds to the closed trajectories.

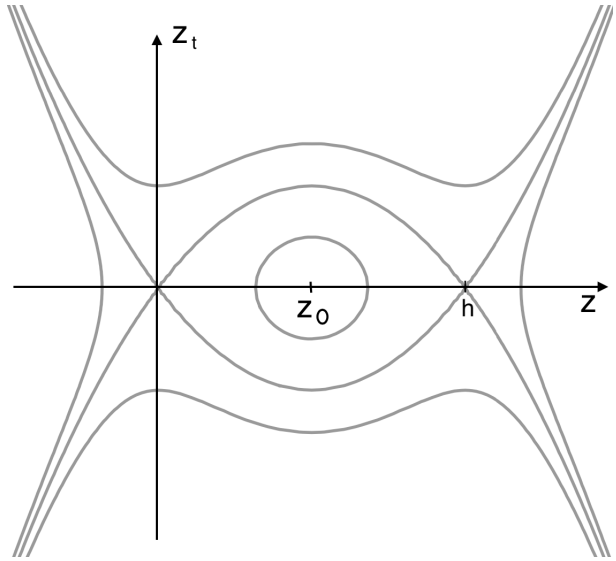

Fig 7. Phase portrait to Eq. (18)

7 Duffing equation with the viscosity and the excitation force

7.1 Motivation

Approximation by a homogeneous equation with zero viscosity does not take into account the asymmetry caused by damping and excitation forces. For example, Figure 8

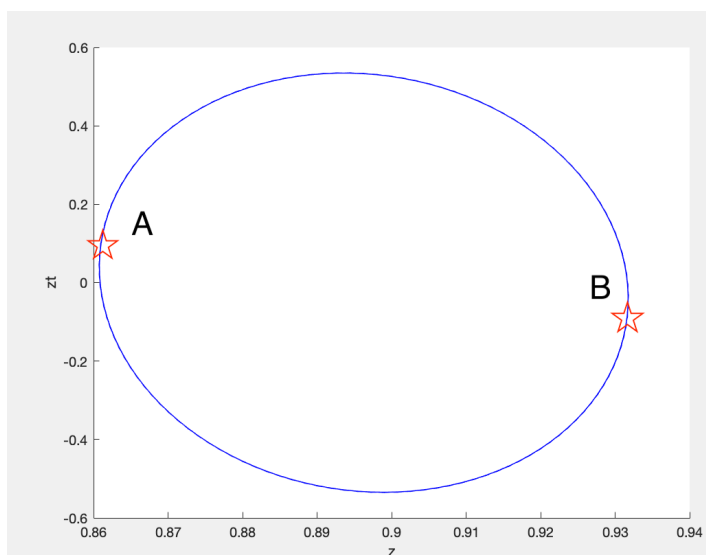

Fig 8. The absolute value of the slope AB multiplied by mass m is the viscosity ν

shows a smoothed data curve for a running participant (10 km/hr, FFT threshold=0.3) in the phase plane (z, z_t). This curve is close to an ellipse, and the absolute value of the slope of the main axis of the ellipse, AB, is equal to $v = \frac{\nu}{m}$ if we assume that the viscosity is a constant. (If the viscosity $\nu = 0$, the slope is vanishing, and the corresponding axis is horizontal.) The symmetry with respect to $z_t = 0$ is disturbed by

this slope.

Now we compare this slightly asymmetrical typical data curve with the symmetrical energy level curves, see Figure 9. Solutions of Eq. (18) with different initial values of z

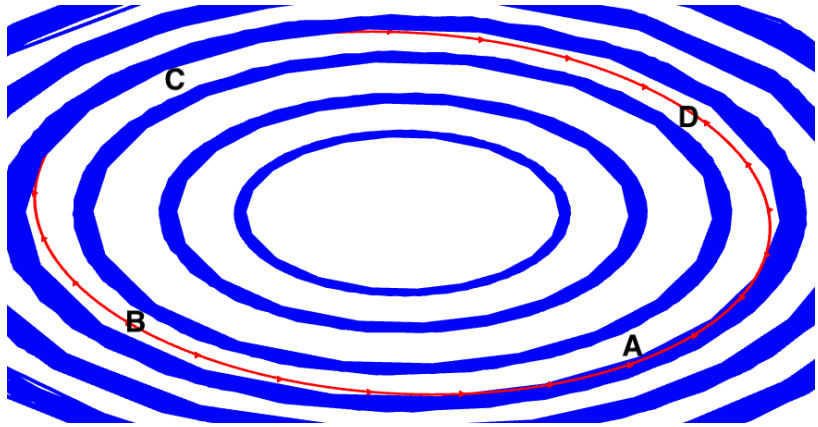

Fig 9. The energy level curves and the data curve (red) in the phase plane (z, z_t). The horizontal axis is the z-axis

$(z_t = 0)$ give a set of energy level curves. The red curve is the data curve, the movement occurs in the direction ABCD. Energy is gained twice in each cycle (gait) in a phase of a "step", BC, and in a phase of a "fall" (in general not the free fall!), DA. The maximum of the energy occurs when the red curve is close to the yellow energy curve (points A and C), the minimum occurs when the red curve is close to the orange energy level (points B and D). There is a natural desire to find an approximation that considers the viscosity and the restoring force.

7.2 Looking for the best fitting curve

We were looking for the best fitting curve in different forms, as for example $z_{tt} + vz_t + C_1 z + C_2 z^2 + C_3 z^3 = f\cos(\Omega t - \varphi)$, where the term vz_t is the linear approximation of the damping force divided by mass, C_1, C_2, and C_3 are coefficients of the cubic nonlinearity. The constant $f = \frac{F}{m}$, where F is the amplitude of the excitation force and m is the mass, Ω is the angular frequency of the excitation force. The gravitation constant g is involved in the equation in a similar way as for the two already discussed models. We have also tried to find the best fitting curve in the forms based on Eqs. (18), (24). As in the previous models, the equation for the best fitting curve was interpreted as a second order differential equation. The solution of the equation was computed and plotted in the same system of coordinates as the data curve. The balance between the viscosity and excitation force was too delicate, and most solution curves became stable spirals. Setting the FFT threshold to 0.5, the balance worked at least for some of the curves based on Eq. (24),

$$z_{tt} + vz_t + kz_0^2(z - z_0) - k(z - z_0)^3 = f\cos(\Omega t - \varphi). \tag{28}$$

7.3 Example

In Figure 10 the red data curve is approximated by a homogeneous differential Eq. (18) (blue curve), and by Eq. (28) containing the damping and restoring forces (green curve). The mean squared error for the homogeneous equation is 0.01. The non-homogeneous equation gives a better approximation with the mean squared error 0.002.

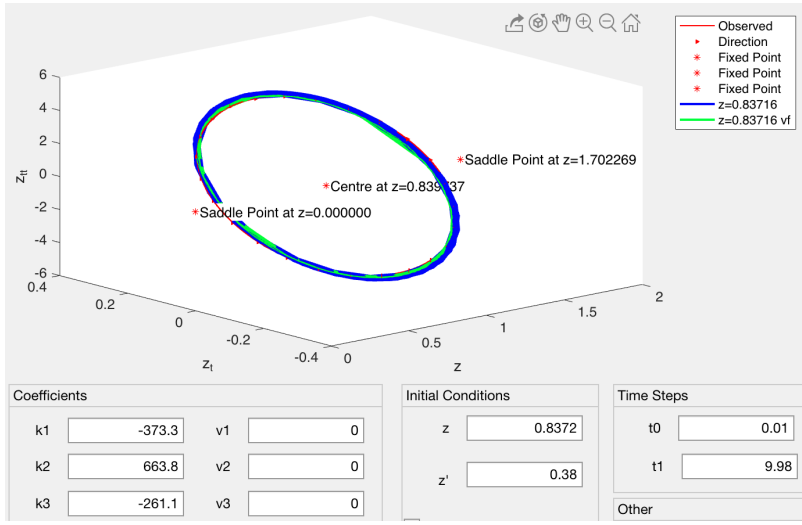

Fig 10. The data curve (red) is approximated by a second order homogeneous differential equation (blue) with the mean squared error 0.01, and by a second order non-homogeneous differential equation (green) with the mean squared error 0.002

8 Plans for future research

8.1 Classification of curves

One of the ideas for future research is to compare and classify the curves for different participants. The curves can have individual features, see for example Figure 11 (FFT threshold 0.03).

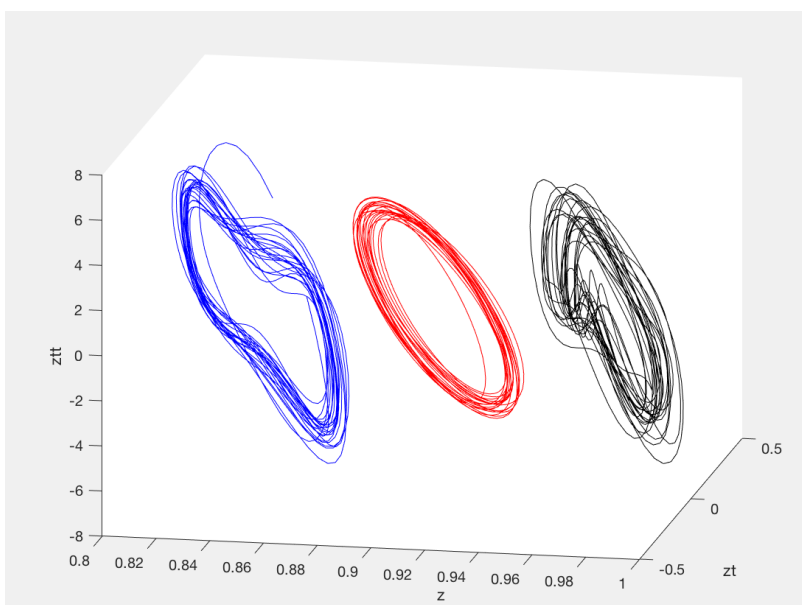

Fig 11. Comparison of curves for three participants walking at 6 km/hr

Also the left and right leg strides are almost indistinguishable if we chose the FFT threshold ≥ 0.3. But for some participants, we observe a difference in the slopes for even and odd strides if the FFT threshold is smaller, suggesting sensitivity in

identification of gait asymmetries. In Figure 12 the green curve (FFT threshold = 0.03) is split into two parts. Recall that different slopes correspond to different angular frequencies. The black curve shows the same data smoothed with an FFT threshold of 0.3. Bipedal models were investigated using a rather mechanical approach in several papers as for example in [14, 20].

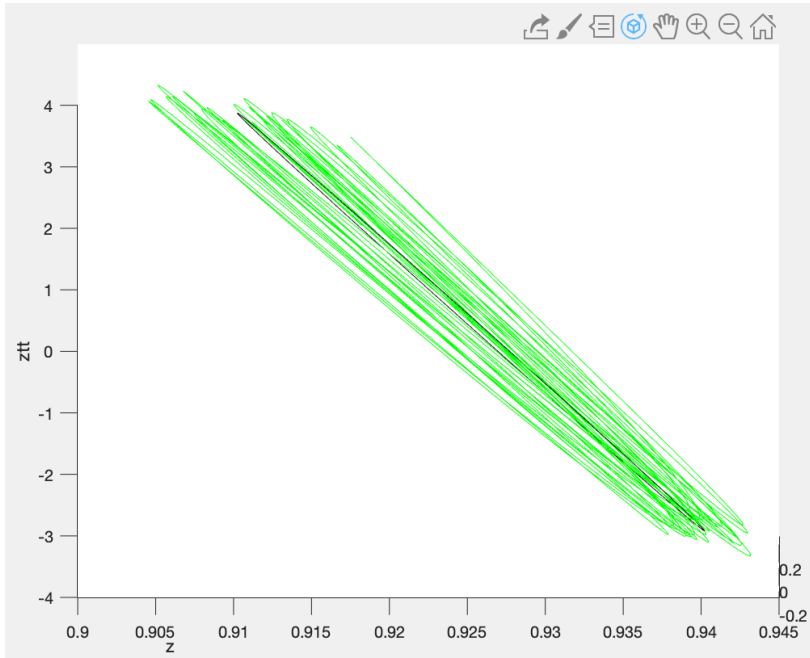

Fig 12. Two curves for a participant walking 6 km/hr. The green curve for FFT threshold 0.03, the black curve for FFT threshold 0.3

8.2 Horizontal components

In this paper we have modelled only the vertical component of the movement of the COM. We plan also to investigate the horizontal components in the future. Our hypothesis is that the horizontal component that is perpendicular to the forward movement, can be approximated by a second order differential equation with negative stiffness,

$$y_{tt} = K_y y(y^2 - s^2). \tag{29}$$

The positions s and $-s$ correspond to the equilibrium points for the left and the right leg, correspondingly, and the origin $y = 0$ is chosen in the middle. K_y is a positive constant. The fixed points for this equations are the saddle point $y = 0$ and two centres $y = \pm s$, see Figure 13. If there is no external or damping force, the y-coordinate of the COM would move along one of the energy curves. Similar to in Figure 9, the external force pushes the point to a level curve that corresponds to a larger energy, and the damping force results a loss of energy.

8.3 Investigating possible reasons for injuries

Our model gives an insight into the dynamics of human gait. We plan to investigate possible reasons for injuries by determining how the stress is generated. One possible idea is to investigate why female runners have more frequent ACL (anterior cruciate ligament) tears than men [25].

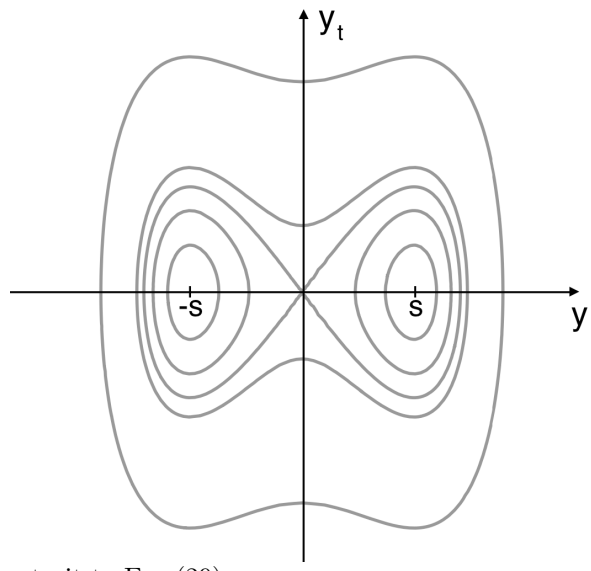

Fig 13. Phase portrait to Eq. (29)

9 Conclusion

We have introduced an innovative method for the investigation of human gait. This method is based on the visualisation of the vertical component of the movement of the centre of mass during walking or running, in the space of the coordinates position, velocity, and acceleration of the centre of mass. This method allows us to compute leg stiffness for an established harmonic oscillator model in a new way, as the slope of the best fitting plane. We determined some differences and some common features for walking and running curves. In this paper we concentrated on features that are common for walking and for running. We suggested a model by a non-linear homogeneous differential equation. For this model we need to know the height of the person, h, during the gait motion, and a coefficient K that depends on a participant and on a walking/running speed. Assuming $z_0 = \frac{1}{2}h$,

$$mz_{tt} + Kz_0^2(z - z_0) - K(z - z_0)^3 = 0. \tag{30}$$

We have a partial success in approximation of the movement by a second order non-linear non-homogeneous equation

$$mz_{tt} + \nu z_t + Kz_0^2(z - z_0) - K(z - z_0)^3 = F\cos(\Omega t - \varphi). \tag{31}$$

We believe that our new method is a tool that leads to other interesting and new results.

10 Acknowledgements

The study followed ethical protocols as per ethics requirements (HE19- 239). Thanks to computer science students Ben Fisk, Danielle Galvin and Jarra McIntyre for developing a prototype of the software used for this paper and to sport science student Megan Bancks for the literature research. Thanks to Adam Harris and Gerd Schmalz for their critical comments and support.

References

1. Bullimore SR, Burn JF. Consequences of forward translation of the point of force application for the mechanics of running. Journal of Theoretical Biology. 2006;238:211–219.

2. Lipfert SW, Gunther M, Renjewski D, Grimmer S, Seyfarth A. A model-experiment comparison of system dynamics for human walking and running. Journal of Theoretical Biology. 2012;292:11–17.

3. Blickhan R. The spring-mass model for running and hopping. Journal of Biomechanics. 1989;22(11):1217–1227. doi:https://doi.org/10.1016/0021-9290(89)90224-8.

4. Blum Y, Lipfert SW, Seyfarth A. Effective leg stiffness in running. Journal of Biomechanics. 2009;42(14):2400–2405. doi:https://doi.org/10.1016/j.jbiomech.2009.06.040.

5. Ferris DP, Louie M, Farley CT. Running in the real world: adjusting leg stiffness for different surfaces. Proceedings of the Royal Society B: Biological Sciences. 1998;265(1400):989–994.

6. Nikooyan AA, Zadpoor AA. Mass–spring–damper modelling of the human body to study running and hopping – an overview. Proceedings of the Institution of Mechanical Engineers, Part H: Journal of Engineering in Medicine. 2011;225(12):1121–1135. doi:10.1177/0954411911424210.

7. Silder A, Besier T, Delp SL. Running with a load increases leg stiffness. Journal of Biomechanics. 2015;48(6):1003–1008. doi:10.1016/j.jbiomech.2015.01.051.

8. Bullimore SR, Burn JF. Ability of the planar spring–mass model to predict mechanical parameters in running humans. Journal of Theoretical Biology. 2007;248(4):686–695. doi:https://doi.org/10.1016/j.jtbi.2007.06.004.

9. Farley CT, González O. Leg stiffness and stride frequency in human running. Journal of Biomechanics. 1996;29(2):181–186. doi:https://doi.org/10.1016/0021-9290(95)00029-1.

10. Dalleau G, Belli A, Bourdin M, Lacour JR. The spring-mass model and the energy cost of treadmill running. European Journal of Applied Physiology and Occupational Physiology. 1998;77(3):257–263. doi:10.1007/s004210050330.

11. Kuo AD. Stabilization of Lateral Motion in Passive Dynamic Walking. The International Journal of Robotics Research. 1999;18((9)):917–930.

12. Donelan JM, Kram R, Kuo AD. Simultaneous positive and negative external and mechanical work in human walking. Journal of Biomechanics. 2002;35:117–124.

13. Mochon S, McMahon TA. Ballistic Walking. Journal of Biomechanics. 1980;13(1):49–57.

14. Geyer H, Seyfarth A, Blickhan R. Compliant leg behaviour explains basic dynamics of walking and running. Proc Biol Sci. 2006;273(1603):2861-2867. doi:10.1098/rspb.2006.3637. Proc Biol Sci. 2006;273(1603):2861–2867.

15. Hong H, Kim S, Kim C, Lee S, Park S. Spring-like gait mechanics observed during walking in both young and older adults. Journal of Biomechanics. 2013;46:77–82.

16. Jung CK, Park S. Compliant bipedal model with the centre of pressure excursion associated with the oscillatory behaviour of the centre of mass reproduces the human gait dynamics. Journal of Biomechanics. 2014;47(223-229).

17. Kim S, Park S. Leg stiffness increased with speed to modulate gait frequency and propulsion energy. Journal of Biomechanics. 2011;44:1253–1258.

18. Song H, Park H, Park S. A springy pendulum could describe the swing leg kinetics of human walking. Journal of Biomechanics. 2016;49:1504–1509.

19. Ludwig C, Grimmer S, Seyfarth A, Maus HM. Multiple-step model-experiment matching allows precise definition of dynamical leg parameters in human running. Journal of Biomechanics. 2012;45:2472–2475.

20. Maus HM, Revzen S, Guckenheimer J, Ludwig C, Reger J, Seyfarth A. Constructing predictive models of human running. J R Soc Interface. 2015;12.

21. Boyce WE, DiPrima RC. Elementary Differential Equations and Boundary Value Problems. seventh edition ed. John Wiley and Sons. Inc; 2001.

22. Jordan D, Smith P. Nonlinear Ordinary Differential Equations. fourth edition ed. Oxford University Press; 2007.

23. Hook R. Micrographia: or, Some Physiological Descriptions of Minute Bodies Made by Magnifying Glasses, With Observations and Inquiries Thereupon. London: Printed by J. Martyn and J. Allestry; 1665.

24. Brennan MJ, Kovacic I. The Duffing Equation: Nonlinear Oscillators and their Behaviour. John Wiley and Sons; 2011.

25. Stefani R. Kinesiology Analysis of Athletics at the Ancient Olympics and of Performance Differences Between Male and Female Olympic Champions at the Modern Games in Running, Swimming and Rowing. Athens Journal of Sports. 2017;4(2):123–138.